

For citation information please see <http://www.claisse.info/Publish.htm>

Determination of the transport properties of a blended concrete from its electrical properties measured during a migration test

J. Lizarazo-Marriaga* and P. Claisse†

Universidad Nacional, Bogotá; Coventry University

The Nernst–Planck equation describes ionic movements in saturated porous materials subject to chemical concentration gradients in the pore fluid and applied electric fields. When applied to a macroscopic system the equation supposes that the flux of each ion is independent of every other one. However, owing to the ionic exchange among different or similar species, there are ionic potentials that affect the final flux. These will distort the applied electric field and thus keep the electroneutrality of the sum of all the ionic species involved. The applied potential will fall linearly across the sample but an additional ‘membrane’ potential will change with position and time. This paper summarises a theoretical and experimental investigation into the application of the non-linear electric membrane potential to the simulation of the migration of chlorides in concrete. A new electrochemical test has been developed and carried out with different samples of concrete blended with pulverised fuel ash (PFA) and ground granulated blastfurnace slag (GGBS). During the tests the transient current and the electrical membrane potential were measured. A numerical model developed previously using the classical equations, but including changes in the concrete membrane potential, was optimised using an artificial neural network (ANN). Based on the experimental results and the simulations, the intrinsic diffusion coefficients of chloride, hydroxide, sodium and potassium were obtained. Also, the initial hydroxide composition of the pore solution, the porosity, and the chloride binding capacity were determined. The results showed good agreement with the theory and can help to explain the complex phenomena that occur during a concrete migration test.

Introduction

Chloride penetration in reinforced concrete is a major concern because of the deterioration of the steel. The resistance to chloride transport can be determined with diffusion tests but these take a long time. The diffusion tests are accelerated by the application of an electrical potential gradient (migration tests) in order to save time. Under the influence of an electric field, ions experience a force directing them towards the electrode that is charged oppositely to the charge on the ion (Bockris and Reddy, 1998). The time needed to per-

form a pure diffusion test may be months; however, a migration test can be completed in just days or hours.

For fully saturated concrete samples with a difference in the concentration of ions in different regions and a constant applied electric potential as in the rapid chloride permeability test (RCPT) (ASTM, 2005) or NT-492 (NORDTEST, 1999), the total flux J_i for each species in the system must be the sum of the migration flux $(J_M)_i$ and the diffusion flux $(J_D)_i$

$$J_i = (J_M)_i + (J_D)_i \quad (1)$$

The general law governing the ionic movements in concrete due to the chemical and electrical potential (Andrade, 1993) is known as the Nernst–Planck equation

$$J_i = D_i \frac{\partial c_i}{\partial x} + \frac{z_i F}{RT} D_i c_i \frac{\partial E}{\partial x} \quad (2)$$

where c_i is the ionic concentration of species i in the pore fluid; x is the distance; z_i is the electrical charge

* Departamento de Ingeniería Civil, Universidad Nacional, Bogotá, Colombia

† Materials Applied Research Group, Coventry University CV1 5FB, UK

(MACR 800152). Paper received on 5 September 2008; last revised 22 June 2009; accepted 11 September 2009

of species i ; F is the Faraday constant; E is the electrical potential; $\delta E/\delta x$ is the electrical field; J_i is the flux of species i ; D_i is the diffusion coefficient of species i ; R is the gas constant; and T is absolute temperature.

When applied to a macroscopic system the Nernst–Planck equation supposes that the flux of each ion is independent of every other one; however, owing to ion–ion interactions there are electrostatic fields that affect the final flux. The drift of a species i is affected by the flows of other species present. The law of electroneutrality ensures that no excess of charge is introduced to the system (Bockris and Reddy, 1998). In a concrete migration test, the current into any point will equal the current out of it (Kirchoff’s law). An increase of concentrations at specific points in the sample can lead to a variation in the electric field. A variation in the electric field can in turn lead to a variation in the flux of each ion.

As a result of the ion–ion interactions, the electrical field contained in the term for the migration flux does not depend only on the constant external electrical potential applied (φ); it is also related to the electrical membrane potential which is formed when various charged species have different mobility. At the start of the test the electrical field is uniform across the concrete; however, when the different ions start to migrate owing to the external voltage applied, they cannot move freely. They are charged particles and interact with species of opposite signs. Owing to the membrane potential a few seconds after the test has started the electrical field is no longer constant. This non-linearity of the electric field is due to the membrane potential gradient and it is equivalent to the liquid junction potential (Lorente *et al.*, 2007) in a concrete migration test. Equation 3 shows the ionic and the membrane potentials for the electrical field. A more complex expression can be found if the Nernst–Planck equation includes a chemical activity coefficient (γ) (Truc, 2000). However, it has been proven that the activity term does not increase the accuracy of the results in a concrete migration test (Samson *et al.*, 2003; Tang, 1999).

$$\frac{\partial E}{\partial x} = \frac{\varphi}{x} - \frac{RT}{F} \frac{\sum_i z_i D_i \frac{\partial c_i}{\partial x}}{\sum_i z_i^2 D_i c_i} \quad (3)$$

Different approaches have been proposed in order to simulate the penetration of chloride during a migration test accounting for all the species and an external electrical driving force. In the references (Claisse and Beresford, 1997; Khitab *et al.*, 2005; Krabbenhoft and Krabbenhoft, 2008; Lorente *et al.*, 2007; Narsilio *et al.*, 2007; Sugiyama *et al.*, 2003; Truc *et al.*, 2000) the Nernst–Planck equation has been used as the way to find the flux of ions and the transport properties of

chlorides in concrete. Some researchers have used it coupled either to the conservation equation or accounting for the distribution and evolution of the electrical field.

In order to determine and understand the penetration of chlorides through concrete, a theoretical and experimental investigation has been carried out. An electrochemical migration test has been developed to determine the electrical membrane potential in laboratory concrete samples by measuring the potential within the samples (Lizarazo-Marriaga and Claisse, 2009). Ordinary Portland concrete (OPC) mixes blended with pulverised fuel ash (PFA) and granulated ground blast-furnace slag (GGBS) have been cast and the transient current and the electrical membrane potential were measured under controlled conditions. A numerical model developed previously (Claisse and Beresford, 1997) using the classical equations, but including changes in the concrete membrane potential distribution, was optimised using an artificial neural network (ANN) model. The new integrated computational model combines a numerical approach to solve the physical problem of electrodiffusion and an artificial intelligence approach to optimise the numerical and experimental results. The outputs of the model yielded the intrinsic diffusion coefficients of chloride, hydroxide, sodium and potassium. The hydroxide composition of the pore solution, the porosity and the chloride capacity of binding were also determined.

Experimental investigation

Test details

The tests carried out as part of this research are summarised in the following section. Each test was run twice and the result shown is the average of both results

Rapid chloride permeability test (RCPT) ASTM-C1202-05. For each test, a slice of concrete 50 mm thick and 100 mm in diameter was placed between two cells containing electrodes and 60 V direct current (d.c.) was applied. One of the cells was filled with a 0.30 N NaOH solution and the other cell was filled with a 3.0% NaCl solution. The curved surface of the specimens was coated with epoxy. Before the test the samples were vacuum saturated in conformity with the standard. The total charge in coulombs was calculated as the area under the current–time curve. The volume of each cell reservoir was approximately 200 ml. All tests were carried out in a temperature-controlled room at $21 \pm 2^\circ\text{C}$. During the tests, the temperature was measured continuously.

New procedure for measuring the membrane potential in the ASTM C-1202 test. Salt bridges were added at different points in the concrete sample to

check the voltage distribution across the sample. Holes 4 mm in diameter and 6–9 mm deep were drilled at each point. The salt bridge used was a solution of 0.1 M potassium chloride (KCl) in order to avoid any junction potential at the interface of the salt solution and the pore solution. The voltage was measured using a standard calomel electrode (SCE) relative to the cathode cell. The current through the concrete and the voltage at different points inside the sample were measured continuously each second with a data logger. A high-impedance data logger (20 MΩ) was used in order to avoid drawing any current through the salt bridges. Figure 1 shows the experimental set-up.

For all the tests, the voltage was measured automatically at three different positions across each sample. The target location of these points was the mid-point and the quarter-points. As, at the start of the test, the electric field is linear across the sample, the membrane potential was calculated as the difference between the measured voltage at any time and the initial voltage. In order to avoid the noise found experimentally during the logging of the tests, a commercial curve-fitting software (The MathWorks, 2001) was used. It was found that this noise was substantially reduced by slightly increasing the depths of the drilled holes for the salt bridges. This observation indicates that the noise was caused by the random distribution of aggregate limiting the contact between the salt bridges and the pore volume.

In a previous study, Zhang *et al.* (2002) measured the membrane potential across OPC mortar specimens during a normal diffusion test using reference electrodes and salt bridges immersed in the external cells of

the sample. They found that for different simulated pore solutions the total junction potentials formed between the measurement devices and the simulated pore solution were in the range between –0.8 and –6 mV. Those values were relatively low compared with the membrane potential measured during the migration tests, so the liquid junction potential formed between the salt bridge and the pore solution in the concrete sample was not accounted for in the research reported in this paper.

As the external voltage across the sample was applied from the power supply by copper electrodes immersed into the cell solutions, there was a small potential drop between the electrodes and the surface of the concrete (McGrath and Hooton, 1996). The relationship between the external voltage delivered by the power supply and the voltage between both ends of the sample was measured and corrected for during the simulations.

Chloride penetration. The chloride penetration was measured after each migration test was finished. The procedure used was the colorimetric method of the Nordtest NT Build 492. Each sample was split axially and sprayed with a solution of 0.1 M silver nitrate. After 15 min, a white silver chloride precipitation on the split surface was visible and the penetration depth was measured.

Concrete mixes

Samples of OPC blended with GGBS and PFA in different proportions were prepared with a fixed water/binder ratio of 0.49. The level of replacement was 10, 30 and 50% for each mineral admixture to cement and the amount of water was kept in the range 195–200 kg/m³. The chemical compositions of the materials used were identified using X-ray fluorescence (XRF) and the specific gravity (SG) of admixtures was measured with a helium picnometer (Micromeritics AccuPyc 1330). Results for the composition of the oxides are presented in Table 1.

Table 2 shows the mix designs and the nomenclature used in this study. All the migration tests were made on samples around 100 days old, which were kept in a room with controlled humidity and temperature until the test. According to the water demand of the admixtures and the proportions used, the mixes had different flow properties. In order to avoid affecting the strength

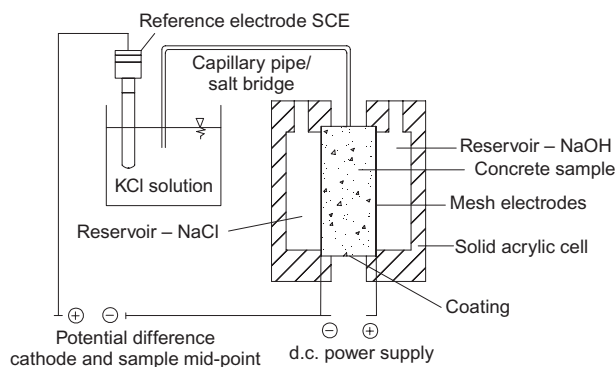


Figure 1. Cell and salt bridge

Table 1. Chemical oxide composition of materials used (*according to the producer)

Binder	Chemical composition: %												SG: g/cm ³
	SiO ₂	TiO ₂	Al ₂ O ₃	Fe ₂ O ₃	MnO	MgO	CaO	Na ₂ O	K ₂ O	P ₂ O ₅	SO ₃	LOI	
OPC*	19.7	–	4.90	2.40	–	2.10	63.30	0.20	0.60	–	2.70	2.7	3.04
GGBS	34.5	0.55	13.16	0.74	0.45	7.75	38.70	0.29	0.55	0.02	1.75	0.7	2.92
FA	47.2	0.96	25.35	9.27	0.05	1.71	2.33	1.52	3.43	0.23	0.48	7.6	2.35

Table 2. Concrete mix design

Mix	w/b ratio	%			Unit content: kg/m ³					
		OPC	FA	GGBS	OPC: kg	PFA: kg	GGBS: kg	Fine agg.: kg	Coarse agg.: kg	Binder: kg
OPC	0.49	100	0	0	394	0	0	692	988	394
10% PFA	0.49	90	10	0	355	39	0	689	984	394
30% PFA	0.49	70	30	0	276	118	0	684	977	394
50% PFA	0.49	50	50	0	197	197	0	678	969	394
10% GGBS	0.49	90	0	10	355	0	39	691	987	394
30% GGBS	0.49	70	0	30	276	0	118	690	986	394
50% GGBS	0.49	50	0	50	197	0	197	690	985	394

because of the differences in the mix compaction, all the mixes were compacted mechanically with a vibrating table. The moulds were filled with concrete in three layers and compacted to remove the air and reach the maximum density.

Modelling

The integrated computational model developed was composed of two main techniques. An electrodiffusion numerical routine was used for calculating the transient current and the mid-point membrane potential during a migration test. This programme uses the physical transport properties as input data. However, as during the test, the physical transport properties are unknown, so a neural network algorithm was trained to optimise those physical properties. As a result of combining both techniques, the transport properties of a concrete sample could be determined when the current and the mid-point membrane potential were measured simultaneously during a migration test.

Numerical electrodiffusion model

The numerical model used in this research was developed in the construction materials applied research group of Coventry university (Claisse and Beresford, 1997). The model works by repeated application of the Nernst–Planck equation through microscopic time and space steps. The effects of the membrane potential in a migration test are applied by distorting the voltage in each space step and checked by ensuring that charge neutrality is maintained throughout the sample at all times for all the ions together. After each time step, adjustments are made to ensure that the total voltage across the sample is correct. The model was able to simulate the transient current during the test, the voltage variation and the membrane potential at each time during the test and in each position. In addition, the model was able to determine the concentration of all the ions used at each time during the test and in each position inside the sample (see Figure 2).

Neural network optimisation model

The network used in this research had a backpropagation algorithm with a multilayer architecture with an input layer of six neurons, a hidden layer of three neurons and an output layer of seven neurons (Figure 3). The six input neurons correspond to the experimental values of current and the mid-point membrane potential through the sample at different times. The output neurons correspond to the intrinsic diffusion coefficients of Cl, OH, Na and K, the porosity, the hydroxide composition into the pore solution at the start of the test, and the binding capacity factor for chloride ions. In the electrodiffusion model the concentration of ions is defined in two ways: the free ions per unit volume of liquid (C_l) and the total ions per unit volume of solid (C_s). The ratio of those concentrations is named the binding capacity factor (α) and it does not have physical units. The neural network model was constructed using the neural network toolbox of Matlab[®].

To train the network, the numerical physical model was run computationally a number of times in order to obtain enough input vectors and the corresponding target vectors. More than 2000 combinations of logical values of transport properties were run with the physical model producing a reliable database to train the neural network. During the training, all the inputs and outputs were normalised between -1 and $+1$ in order to avoid the influence of the scale of the physical quantities. In the same way, a tangential transfer function was limited to be between -1 and $+1$. The Levenberg–Marquardt training algorithm was used.

Integrated numerical–neural network model

The profile and evolution of the membrane potential and the current is associated either with

- factors related to the test, such as the electrical external potential and the chemistry of the external reservoirs cells, or
- factors related to the features of the sample, such as the concentration of species in the pore solution,

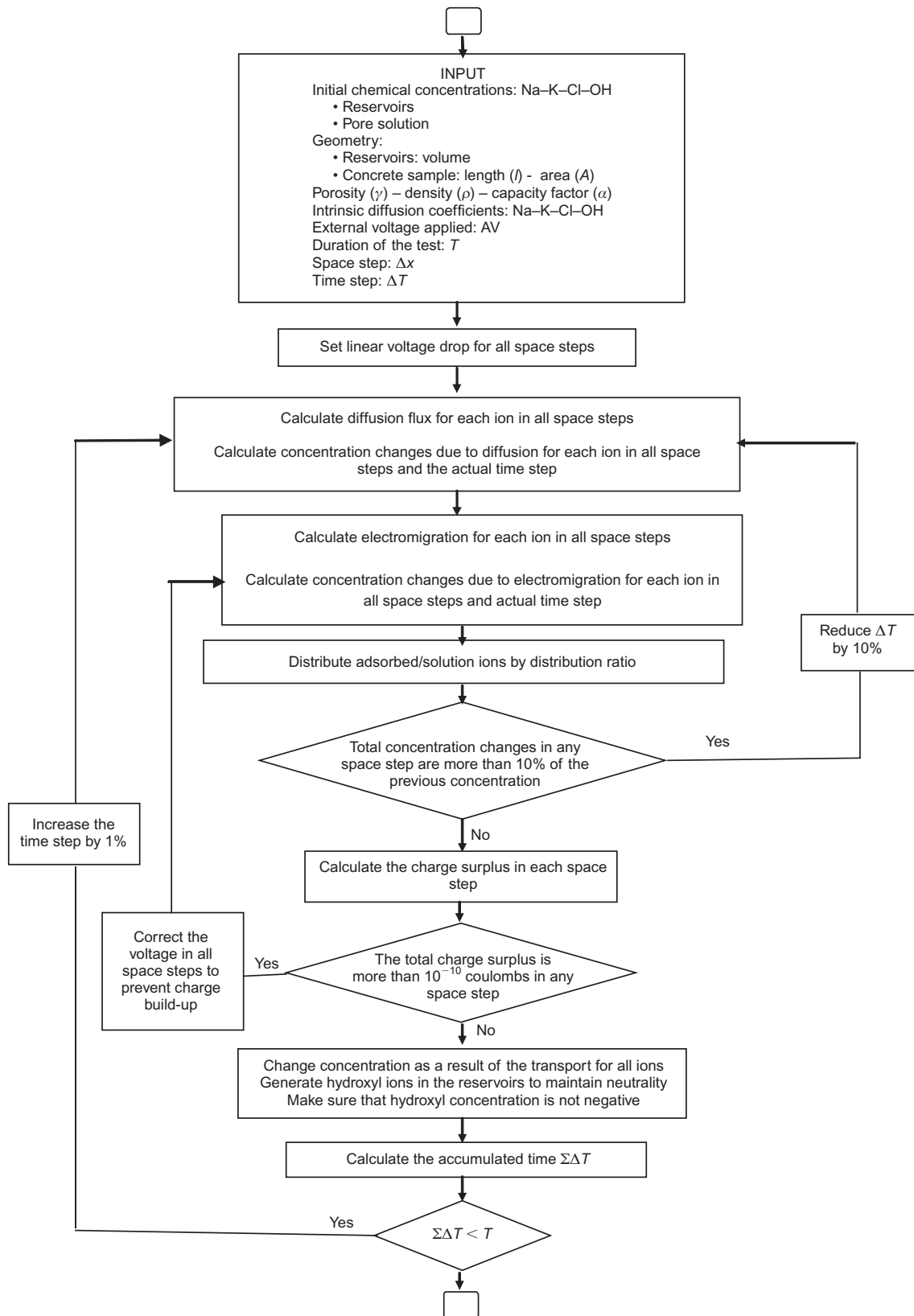


Figure 2. Computer model used in this research

the tortuosity of the pore network, the porosity of concrete, the intrinsic properties of diffusion for each ion present, and the binding capacity or adsorption for each ion.

In the experiments, all the conditions related to the test were carefully controlled and were the same for all mixes. Therefore, it can be argued that the differences in the current and the mid-point membrane potential

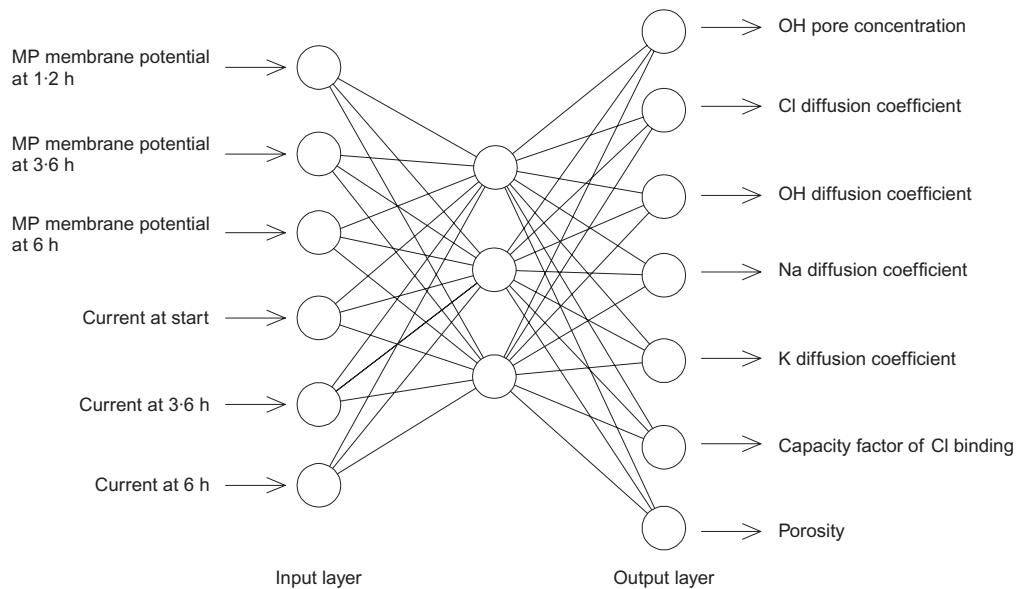


Figure 3. Neural network used

among mixes were due to the differences in the transport characteristics of each mix. When measuring the transient current by itself, it is not possible to determine a unique numerical value for all the concrete transport properties because there are too many unknowns and not enough relationships to solve the system. However, with the simultaneous measurement of the current and the mid-point membrane potential it is possible to determine a unique combination of the transport properties by using the neural network and making the following assumptions.

- (a) Although it is well known that chlorides, hydroxides, sodium and potassium have complex reactions with the cement hydration products, the only ions permitted in the model to have adsorption or binding with the cement matrix were chlorides. The reason for making this assumption was to limit the number of variables to optimise.
- (b) The chloride apparent diffusion coefficients (D_{app-Cl}) were determined from the intrinsic diffusion coefficient (D_{Cl}), the porosity of the material (ϵ), and the binding capacity factor (α) using Equation 4 (Lizarazo-Marriaga and Claisse, 2009).

$$\frac{\alpha}{\epsilon} = \frac{D_{Cl}}{D_{app-Cl}} \quad (4)$$
- (c) As the adsorptions for hydroxides and cations were neglected, the intrinsic and apparent diffusion coefficients were equal for those ions, giving $\alpha/\epsilon = 1$.
- (d) The chloride transport processes into the concrete were restricted by binding with a linear isotherm. Although it has been demonstrated experimentally (Delagrave *et al.*, 1997) that non-linear isotherms better reflect the adsorption phenomena, the model uses an average linear isotherm that represents the average adsorption of chlorides well and allows the

model to have a direct relationship between intrinsic and apparent diffusion coefficients.

- (e) The pore solution at the start of the test does not include chloride ions and the equilibrium for hydroxyl ions was assumed to be maintained at a proportion of 33% of sodium and 66% of potassium. The ratio of potassium to sodium in the starting materials was always 2. This assumption was based on published results (Bertolini *et al.*, 2004).

Test results and discussion

The total electrical charge passed, the chloride penetration during the test, and the evolution of the membrane potential were measured and analysed. Using the integrated computational model, the transport properties of the mixes tested were then found.

Charge and chloride penetration

The final charge passed and the chloride penetration are shown in Table 3. The results indicate that there were great benefits using either GGBS or PFA. The best results were obtained when replacements of 30% of PFA and 50% of GGBS were used. Figure 4 shows a summary of the properties measured relative to the values corresponding to the OPC samples. The addition of either mineral admixture produces a positive effect, reducing the charge and chloride penetration.

Membrane potential

The behaviour of the membrane potential across the sample during the test is shown in Figure 5 as contour graphs for samples OPC, 10% GGBS and 10% PFA; each graph represents the average of two samples. The horizontal axis is the length of the sample: 50 mm, and

Table 3. Properties measured

Mix	OPC	10% PFA	30% PFA	50% PFA	10% GGBS	30% GGBS	50% GGBS
Penetration: mm	5.00	4.20	0.62	0.68	4.45	1.02	0.66
Charge: coulombs	4644	2435	1237	1253	4202	1848	1097

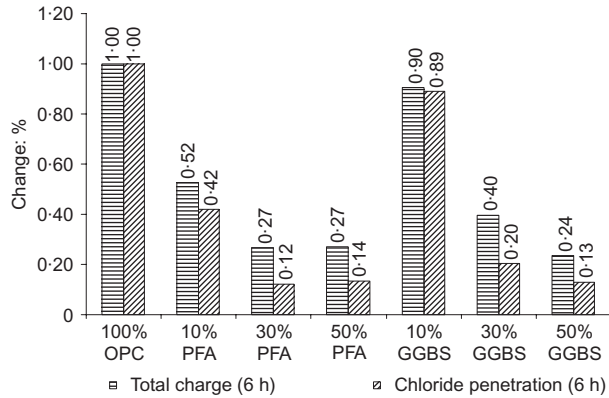


Figure 4. Total charge and chloride penetration (60 V)

the vertical axis is the duration of the experiment: 6 h. The iso-response curves for the membrane potential show that the distribution of the voltage is not linear in time and space during a migration test. For all the contours there is a well-defined area with negative values of voltage (with a total voltage lower than the voltage at the start of the test) or areas with positive values (voltages bigger than the initial external applied voltage). Depending on the type and amount of mineral admixture used, the contour reached either a maximum or a minimum.

The contour plots indicate that, if the amount of admixture is increased, the voltage tends to reach more negative values, especially for the PFA mixes. If the total electrical field is constant in the sample it would be expected that the behaviour of the conductivity would have the same trend as the current. However, as the voltage varies across the sample, the calculated conductivity at any point across the sample is transient in time and position owing to the effect of the membrane potential. This is very important because this effect needs to be included in the general equations of ionic transport in order to predict adequately the chloride penetration.

From the contour plots the membrane potential at any point and time during the test can be examined. This has academic and scientific value. However, such tests are expensive and not easy to complete. As an alternative, it has been proposed to use only the behaviour of the mid-point as a source of additional information. The electric membrane potential at the mid-point for each mix is shown in Figure 6. All mixes showed from the start a sustained decrease, reaching a local minimum and starting again to increase the voltage values.

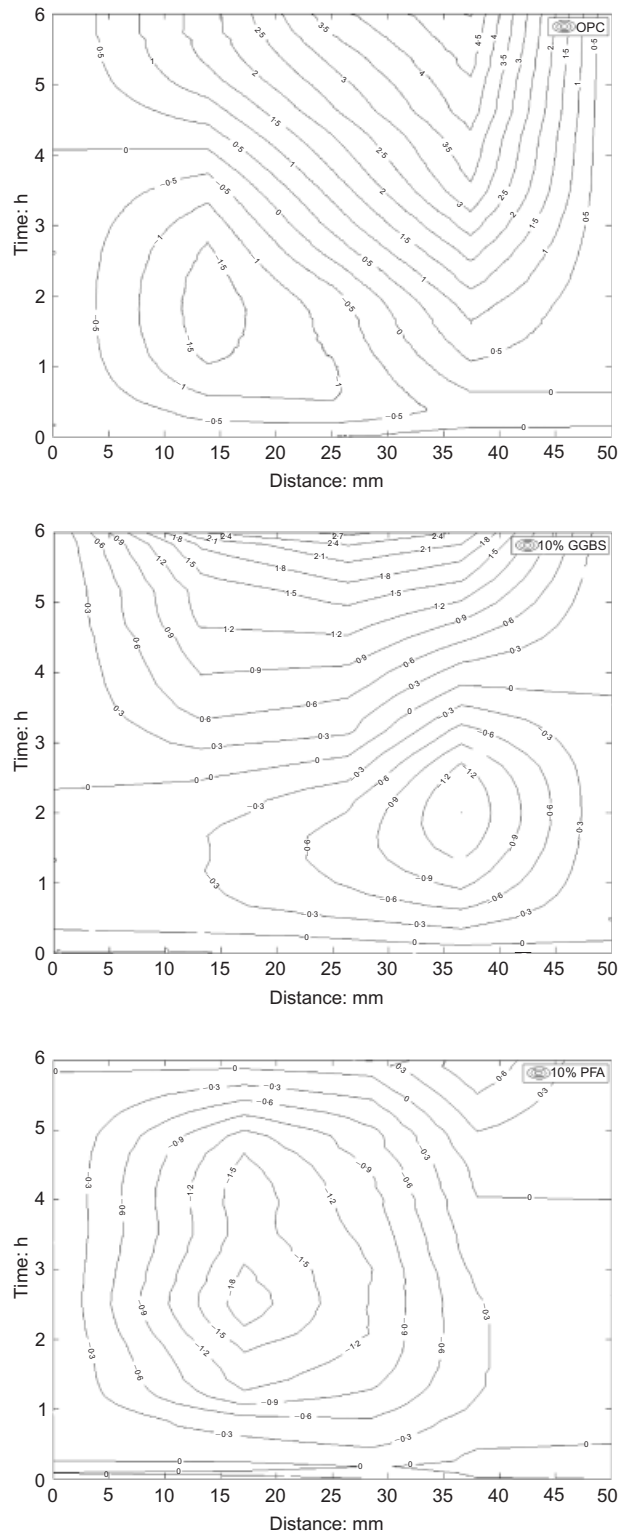


Figure 5. Membrane potential measured

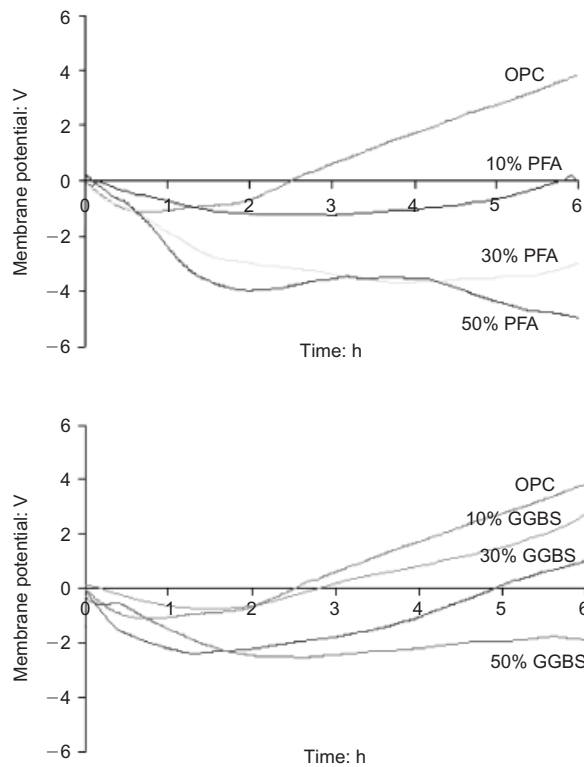


Figure 6. Membrane potential in the mid-point of the samples

Integrated numerical–neural network model

The artificial neural network (ANN) was trained using the results of the model and then used to obtain the transport properties from the experimental results. Table 4 shows the numerical values of the properties obtained for all the mixes. In order to validate the results, the physical numerical model was run again for each mix using as inputs the values obtained from the neural network. As an example, Figure 7 shows the simulated and measured transient currents and mid-point membrane potentials for some of the samples used. From the graphs, it can be concluded that all the simulations are in very good agreement with the experiments, with the simulations for the current better than those for the mid-point voltage.

Transport properties

All the migration tests had non-steady-state conditions because of the characteristics of the experiments in which there were a small volume of external cells, a high external voltage, and a short duration. Although in some mixes it was possible that the chlorides reached the anode (thus giving a uniform condition through the sample), the depletion of the external cells ensured that a steady-state condition was never achieved. Therefore, the estimated Cl^- apparent diffusion coefficient and the intrinsic diffusion coefficients for the other ions in the system are for non-steady-state conditions. Figure 8 shows the calculated apparent coefficients of diffusion. The sodium and potassium coefficients were significantly smaller than the values for chlorides and hydroxides, as observed previously by other researchers (Andrade, 1993; Zhang *et al.*, 2002). These results confirm that the mobility of cations in a porous media is less than the mobility of anions. However, they are absolutely necessary in the simulation. Either in a self-diffusion test or in the presence of an applied voltage gradient across the specimen, the charge electroneutrality is maintained in the code by adjusting the membrane potential at all times. Small changes in the diffusion of cations produce large changes in the mid-point membrane potential. The diffusion coefficients obtained for sodium (D_{Na}) were greater than for potassium (D_{K}); the ratio $D_{\text{Na}}/D_{\text{K}}$ was different depending on the amount and type of admixture. It was found that if there was an increase in the amount of mineral admixture, the ratio $D_{\text{Na}}/D_{\text{K}}$ tended to decrease. Although the coefficient of diffusion for potassium is greater than for sodium in an infinite dilute solution (Bockris and Reddy, 1998), the results of this work showed that for the samples tested this is not always the case because of the ionic exchange among all the ions coming from the external cells and the pore solution. The ratio $D_{\text{Na}}/D_{\text{K}}$ varies for each concrete sample according to all its transport properties including the composition of its pore solution at the start of the test.

The obtained migration diffusion coefficients for chlorides and hydroxides showed that both ions have a

Table 4. Transport properties calculated with the integrated model

	OH conc'n	Intrinsic coefficient, D_{Cl} : m^2/s	Intrinsic coefficient, D_{OH} : m^2/s	Intrinsic coefficient, D_{Na} : m^2/s	Intrinsic coefficient, D_{K} : m^2/s	Factor capacity, Cl	Capillary concrete porosity	Apparent coefficient, $D_{\text{app/Cl}}$: m^2/s
OPC	234.1	1.94×10^{-10}	7.81×10^{-11}	3.52×10^{-11}	1.07×10^{-11}	0.29	0.19	1.25×10^{-10}
10% PFA	223.2	1.09×10^{-10}	3.68×10^{-11}	2.17×10^{-11}	8.21×10^{-12}	0.35	0.18	5.55×10^{-11}
30% PFA	208.6	8.17×10^{-11}	2.56×10^{-11}	1.59×10^{-11}	7.23×10^{-12}	0.41	0.17	3.37×10^{-11}
50% PFA	207.3	1.05×10^{-10}	2.99×10^{-11}	1.60×10^{-11}	8.19×10^{-12}	0.40	0.17	4.42×10^{-11}
10% GGBS	226.0	2.06×10^{-10}	7.66×10^{-11}	3.13×10^{-11}	1.12×10^{-11}	0.30	0.18	1.25×10^{-10}
30% GGBS	199.2	1.00×10^{-10}	3.80×10^{-11}	1.92×10^{-11}	7.71×10^{-12}	0.40	0.17	4.27×10^{-11}
50% GGBS	199.1	9.32×10^{-11}	2.85×10^{-11}	1.52×10^{-11}	7.67×10^{-12}	0.42	0.17	3.65×10^{-11}

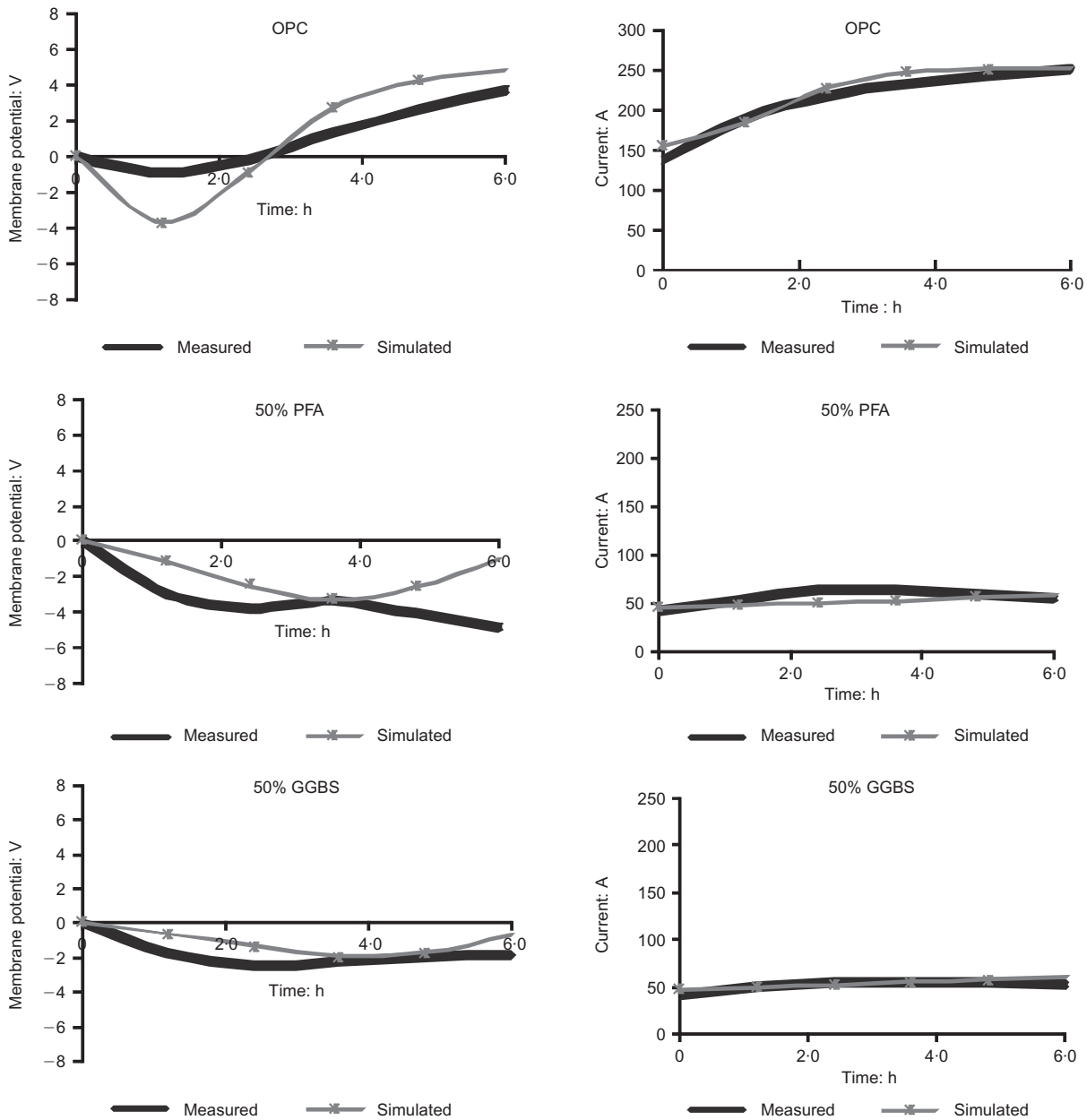


Figure 7. Transient mid-point membrane potential and current, both simulated and measured

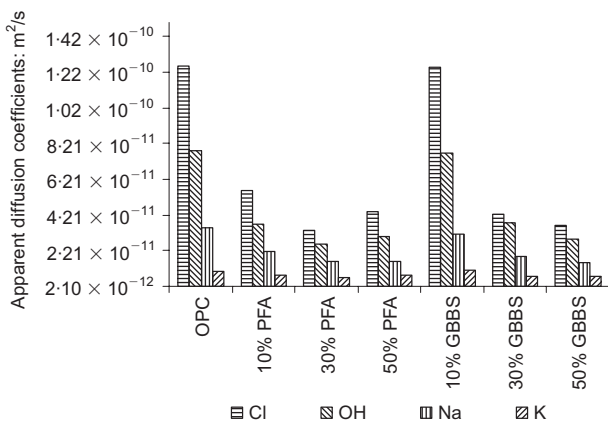


Figure 8. Calculated apparent diffusion coefficients

high mobility and are responsible for most of the transport of charge. However, in contrast with the conclusions of some researchers (Feldman *et al.*, 1994; Zhang *et al.*, 2002) the results of the simulations indicated that the diffusion coefficients of chlorides were greater than the hydroxide coefficients. The numerical values of the apparent chloride coefficients were between 10 and 60% greater than for the hydroxides depending on the level of mineral admixture replacement. With an increase in the amount of either mineral admixture, the ratio D_{app-Cl}/D_{OH} tends to decrease. It is believed that the ratio between the diffusivity of chlorides and hydroxides depends on all the external conditions of the test and all the internal transport properties and features of the concrete and it is not a rule that it is always less than 1.

On the other hand, the calculated apparent diffusion coefficients obtained were relatively high compared with some reported in the literature. Usually, for a concrete of good quality, a chloride diffusion coefficient of the order of 10^{-12} m²/s is expected. However, these differences can be explained through two reasons. First, the water/binder ratio for all the mixes used was just 0.49; this means that the concrete used was not the most impermeable. Second, the diffusion coefficients obtained in this work apply to a multispecies system coupled through the membrane potential, instead of those obtained in experiments and reported in literature where ions are physically affected by the ionic exchange among species, but the coefficients are calculated through equations that account for only single chloride diffusion and no ionic interaction.

The simulated results for the initial composition of the pore solution are shown in Figure 9 as the hydroxide ion (OH⁻) concentration. For the OPC sample, for example, a numerical value of 234 mol/m³ was obtained for hydroxide that corresponds to 78 mol/m³ of sodium and 156 mol/m³ of potassium in order to keep the initial electroneutrality of the system (units are mol per cubic metre of pore solution). With the increase of the amount of mineral admixture, a reduction was found in the initial hydroxide composition of the pore solution as was expected. This has been previously reported by Page and Vennesland (1983). The calculated hydroxide reduction of the solution into the pores for the 30% GGBS blended concrete was around 15% with respect to the OPC, and for the 30% PFA blended concrete was around 10% with respect to the OPC. Above 30% of replacement, there was no further reduction in the hydroxide ion concentration.

From the integrated model, the calculated porosity was found. There was a reduction in the porosity with an increase in the amount of any admixture, and the beneficial effect of GGBS and PFA was greater with mixes of 30% PFA and 50% GGBS respectively. Figure 10 shows the variation of the calculated porosity for different percentages of admixture. In the same way, the calculated chloride capacity factor of binding is shown in Figure 11. It was found that it tends to in-

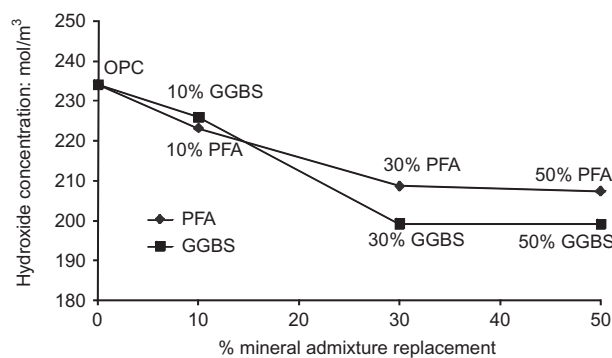


Figure 9. Calculated hydroxide concentration at the start of the test plotted against level of mineral admixture replacement

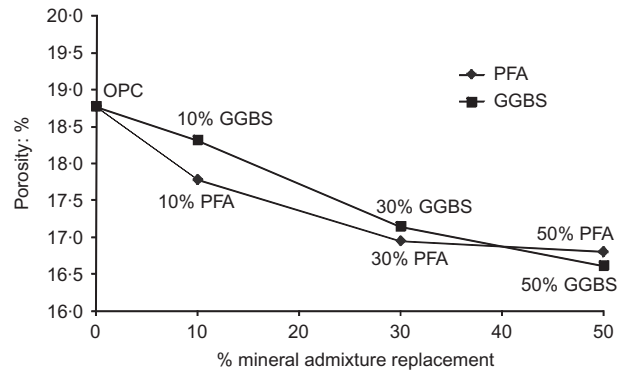


Figure 10. Calculated concrete capillary porosity against mineral admixture level of replacement

crease with an increase in the amount of mineral admixture. The greatest chloride capacity factor was found in the mixes of 30% PFA and 50% GGBS and confirms the optimum percentages for those materials.

Correlation of the estimated chloride diffusion coefficients with the measured charge and penetration

The correlation coefficient *r* between the obtained chloride diffusivity and the chloride penetration after 6 h was calculated in order to find out their association and dependency. Figure 12 shows the regression that fits the best straight line to the data and shows the numerical coefficient of determination *R*², which indi-

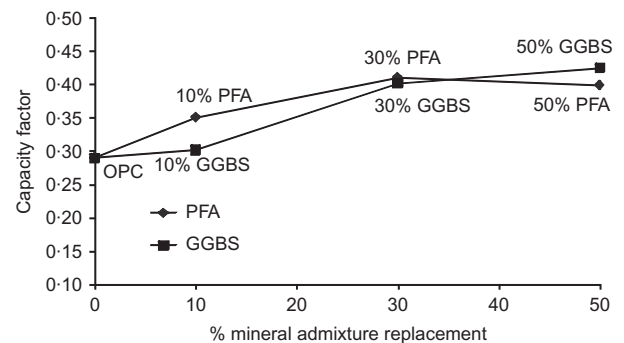


Figure 11. Calculated capacity factor plotted against level of mineral admixture replacement

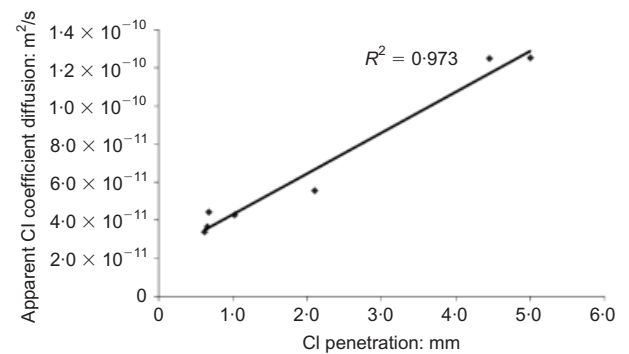


Figure 12. Correlation between the calculated Cl apparent diffusion coefficient and the Cl penetration measured during the test

icates the amount of variability. The value of correlation was $r = 0.99$, and shows that the apparent chloride coefficient of diffusion obtained through the integrated numerical–neural network model is in good agreement with the measured penetration regardless of the mineral admixtures used. From Figure 12, it is argued that for any sample of concrete the information of current obtained from the traditional ASTM C1202 test and the membrane potential obtained from the electrochemical test presented in this paper define together the transport properties of the material. In addition, the numerical values of the diffusion coefficients can be obtained from the computational model proposed.

The relationship between the charge in coulombs obtained from the standard ASTM C1202 test and the calculated chloride diffusion coefficients is shown in Figure 13. The correlation between the charge and the intrinsic (part (a)) and apparent (part (b)) coefficients is shown. The link between both coefficients was defined by Equation 4. The intrinsic coefficient defines the transport of matter when the flux is calculated per unit cross-sectional area of the pores and the concentration in the free liquid. In contrast, the apparent coefficient defines the transport of any ion when the flux is calculated per unit area of the porous material and the average concentration in the material. The reason why both coefficients are presented is because the computer model calculates the intrinsic coefficient, but the apparent coefficients are normally used to predict the service live of concrete structures. From Figure 13(b) it can be seen that the relation charge–apparent chloride coefficient

for GGBS had a very good correlation with a determination coefficient $R^2 = 0.974$. According to this, the equation that defines that relationship can be used as a tool to estimate the apparent diffusion coefficient in m^2/s from the measured value of charge in coulombs for GGBS mixes ($D_{app-GGBS}$) with any level of replacement between 0 and 50%.

$$D_{app-GGBS} = 3 \times 10^{-14} \times \text{charge} - 4 \times 10^{-13} \quad (5)$$

For PFA mixes, the charge and the apparent chloride diffusion coefficient had an acceptable correlation as shown in Figure 13(b); in general terms this shows that the ASTM C1202 test adequately predicts the chloride penetrability in a blended GGBS or PFA concrete. However, it has been reported extensively in the literature that in a migration test the flow of current and the charge passed through the mixtures with mineral admixtures, especially with PFA, is strongly related to the conductivity of the pore fluid within the concrete (Chindaprasirt *et al.*, 2008; Sengul *et al.*, 2005; Wee *et al.*, 2000; Yang and Wang, 2004). As the percentage of any admixture replacement affects the ionic concentration and the conductivity of concrete, Figure 14 shows the correlation between the ratio of chloride diffusivity to charge plotted against percentage of admixture replacement for the intrinsic (Figure 14(a)) and apparent (Figure 14(b)) coefficients. Figure 14(a) shows that the ratio of intrinsic coefficient to charge increases linearly with the increase of the amount of mineral admixtures, especially for PFA which showed a determination coef-

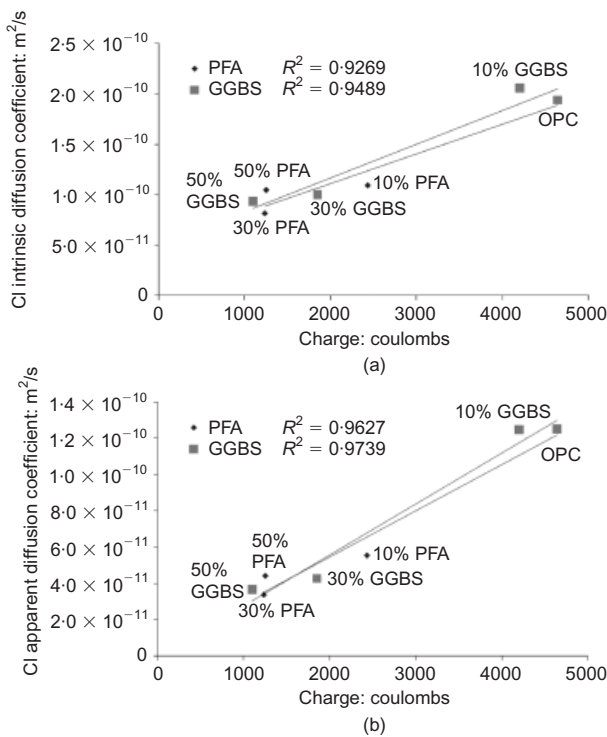


Figure 13. Correlation between diffusion coefficients and charge

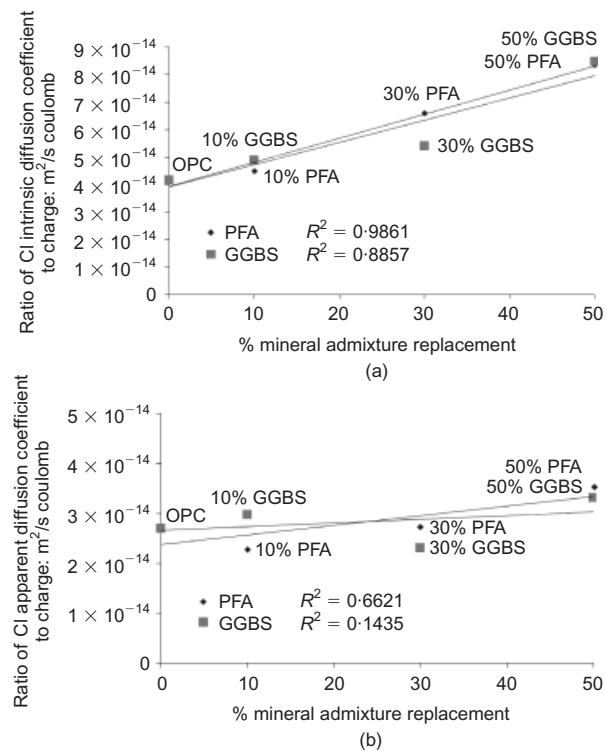


Figure 14. Correlation between diffusion coefficients and mineral admixture replacement

efficient of $R^2 = 0.986$. The chloride intrinsic diffusion coefficient for PFA ($D_{\text{int-PFA}}$) in m^2/s can be obtained from Equation 6 from the measured value of charge in coulombs and the level of PFA as a percentage (%PFA). The apparent coefficient can be calculated from

$$D_{\text{int-PFA}} = [9 \times 10^{-16} \times (\% \text{PFA}) + 4 \times 10^{-14}] \times \text{Charge} \quad (6)$$

In Figure 14(b), the ratio of apparent diffusion to charge plotted against percentage of admixture shows that there is a poor relationship between them, especially for the GGBS mixes. The very good correlation of the ratio of chloride intrinsic diffusion coefficient to charge plotted against percentage of admixture for PFA mixes shows that when this admixture is used it is necessary to correct the charge calculated during the ASTM C1202 in order to obtain more reliable results.

Conclusions

- Measuring the voltage within a sample is a powerful method for obtaining more useful data from migration tests.
- Using ANNs trained on numerical simulations of the migration test yields viable results for the fundamental properties of concrete. The initial hydroxide composition of the pore solution, the chloride binding capacity, the porosity and the diffusion coefficients for all the species involved were estimated with good results.
- Results obtained show that the ratios between sodium and potassium, and chlorides and hydroxides in a migration test do not follow the behaviour of single species in a dilute solution. In the same way, the calculated values of chloride diffusion coefficient were larger than those usually reported in the literature; however, they are in good agreement with the measured chloride penetration.
- This paper presents methods to modify the ASTM C1202 test and obtain far more information about the samples and their potential durability.

Acknowledgements

The authors would like to thank for their support, the Universidad Nacional de Colombia, la fundación para el futuro de Colombia COLFUTURO, and the Programme Alβan (the European Union programme of high-level scholarships for Latin America, scholarship number E06d101124CO).

References

ASTM (American Society for Testing and Materials) (2005) *Standard Test Method for Electrical Indication of Concrete's Ability to Resist*

- Chloride Ion Penetration*. ASTM International, West Conshohocken, PA, ASTM-C1202.
- Andrade C (1993) Calculation of chloride diffusion coefficients in concrete from ionic migration measurements. *Cement and Concrete Research* **23**(3): 724–742.
- Bertolini LBE, Pedefferri P and Polder RB (eds) (2004) *Corrosion of Steel in Concrete: Prevention, Diagnosis, Repair*. Wiley, Chichester.
- Bockris J and Reddy A (1998) *Modern Electrochemistry I Ionics*. Plenum Press, New York.
- Chindaprasit P, Rukzon S and Sirivivatnanon V (2008) Resistance to chloride penetration of blended Portland cement mortar containing palm oil fuel ash, rice husk ash and fly ash. *Construction and Building Materials* **22**(5): 932–938.
- Claisse PA and Beresford TW (1997) *Obtaining More from the Electrical Chloride Test*. American Concrete Institute, Farmington Hills, MI, ACI-SP 170, 170–57 1119–1132.
- Delagrave A, Bigas JP, Ollivier JP, Marchand J and Pigeon M (1997) Influence of the interfacial zone on the chloride diffusivity of mortars. *Advanced Cement Based Materials* **5**(3): 86–92.
- Feldman RF, Chan GW, Brousseau RJ and Tumidajski PJ (1994) Investigation of the rapid chloride permeability test. *ACI Materials Journal* **91**(2): 246–255.
- Khitab A, Lorente S. and Ollivier JP (2005) Predictive model for chloride penetration through concrete. *Magazine of Concrete Research* **57**(9): 511–520.
- Krabbenhoft K and Krabbenhoft J (2008) Application of the Poisson–Nernst–Planck equations to the migration test. *Cement and Concrete Research* **38**(1): 77–88.
- Lizarazo-Marriaga J and Claisse P (2009) Effect of the non-linear membrane potential on the migration of ionic species in concrete. *Electrochimica Acta* **54**(10): 2761–2769.
- Lorente S, Voinitchi D, Bégué-Escaffit P and Bourbon X (2007) The single-valued diffusion coefficient for ionic diffusion through porous media. *Journal of Applied Physics* **101**(2): 024907.
- McGrath PF and Hooton RD (1996) Influence of voltage on chloride diffusion coefficients from chloride migration tests. *Cement and Concrete Research* **26**(8): 1239–1244.
- Narsilio GA, Li R, Pivonka P and Smith DW (2007) Comparative study of methods used to estimate ionic diffusion coefficients using migration tests. *Cement and Concrete Research* **37**(8): 1152–1163.
- NORDTEST (1999) *Concrete, Mortar and Cement-based Repair Materials: Chloride Migration Coefficient from Non-steady-state Migration Experiments*. NORDTEST, Esbo, Finland, NTBUILD-492 NORDTEST method.
- Page CL and Vennesland O (1983) Pore solution composition and chloride binding capacity of silica-fume cement pastes. *Materials and Structures* **16**(1): 19–25.
- Samson E, Marchand J and Snyder KA (2003) Calculation of ionic diffusion coefficients on the basis of migration test results. *Materials and Structures* **36**(3): 156–165.
- Sengul O, Tasdemir C and Tasdemir MA (2005) Mechanical properties and rapid chloride permeability of concretes with ground fly ash. *ACI Materials Journal* **102**(6): 414–421.
- Sugiyama T, Ritthichauy W and Tsuji Y (2003) Simultaneous transport of chloride and calcium ions in hydrated cement systems. *Journal of Advanced Concrete Technology* **1**(2): 127–138.
- Tang L (1999) Concentration dependence of diffusion and migration of chloride ions: Part 2. Experimental evaluations. *Cement and Concrete Research* **29**(9): 1469–1474.
- The MathWorks (2001) *I. Curve Fitting Toolbox – For Use With MATLAB*. The MathWorks, Inc., Natick, MA.
- Truc O (2000) *Prediction of Chloride Penetration into Saturated Concrete – Multi-species Approach*. PhD thesis, Chalmers University, Göteborg, Sweden.
- Truc O, Ollivier J-P and Nilsson L-O (2000) Numerical simulation of multi-species transport through saturated concrete during a migration test – MsDiff code. *Cement and Concrete Research* **30**(10): 1581–1592.

Wee TH, Suryavanshi AK and Tin SS (2000) Evaluation of rapid chloride permeability test (RCPT) results for concrete containing mineral admixtures. *ACI Materials Journal* **97(2)**: 221–232.

Yang CC and Wang LC (2004) The diffusion characteristic of concrete with mineral admixtures between salt ponding test and accelerated chloride migration test. *Materials Chemistry and Physics* **85(2–3)**: 266–272.

Zhang JZ, Li J and Buenfeld NR (2002) Measurement and modelling of membrane potentials across OPC mortar specimens between 0.5 M NaCl and simulated pore solutions. *Cement and Concrete Composites* **24(5)**: 451–455.

Discussion contributions on this paper should reach the editor by 1 September 2010